Large-Signal Characterization of Coupled RF Amplifiers for Parallel Transmit

Michael Twieg[1] and Mark A Griswold[1,2]

[1]Dept. of Electrical Engineering and Computer Science, Case Western Reserve University, Cleveland, OH, United States, [2]Dept. of Radiology, Case Western Reserve University, Cleveland, OH, United States

Target audience: This work is relevant to those interested in parallel transmit amplifiers.

Purpose: Previous work[1,2] has demonstrated the use of high efficiency switch mode power amplifier (SMPA) topologies for miniature on-coil amplifiers aimed at use in parallel transmit coil arrays. Though such amplifiers demonstrate very high efficiency and power density in isolation, there has not yet been any detailed quantification of how these amplifiers behave when the RF coils are coupled to each other, primarily due to their relatively complex behavior. Linear power amplifiers (LPA) are normally assumed to be time invariant, homogeneous, and additive, making them simpler to model using linearized parameters such as transconductance, complex impedance, and scattering parameters. SMPA topologies, such as the Current Mode Class D (CMCD) topology shown in fig 1, are different in that they are inherently periodically-time-varying systems, and they show strong nonlinear behavior. To address these issues, we have developed a method for experimentally quantifying the effective open loop output impedance and power efficiency of coupled power amplifier topologies across their full control space, and we demonstrate its application to the CMCD topology.

Methods: *CMCD coupling model:* The coupling phenomenon observed in coil arrays is due to magnetic and electric fields from one coil element inducing an electromotive force ε in neighboring coils[3]. This work focuses solely on the role of magnetic flux coupling, described by k_m between two coils with inductances L_1 and L_2. The ε_{21} inducted in coil L_1 by current I_{L2} in coil L_2 is given by $\varepsilon_{21}=j\omega I_{L2}k_m\sqrt{L_1L_2}$. This ε_{21} will alter the current in coil L_1 according to $\Delta I_{L1}=\varepsilon_{21}/(Z_{amp1}+Z_{C1})$ where Z_{C1} is the total impedance of coil 1 at f_0 and Z_{amp1} is the effective output impedance of amplifier 1. Fig 1 shows a simple model of this phenomenon as it occurs in a single CMCD amplifier. *CMCD coupling measurement:* We constructed two transmit channels (CH1 and CH2) consisting of RF amplifiers and RF coils for operation at 10 MHz. The relatively low frequency was chosen to emphasize the amplifier's inherent behavior while mitigating other complicating factors that may be more relevant at higher frequencies. CH1 used a CMCD topology, while CH2 used a VMCD topology. A π/2 phase shifter was placed at the output of CH2 to increase its output impedance. Each amplifier was biased by a buck converter whose duty cycle was controlled by an external control voltage. The DC output current and voltage of the buck converters were also monitored. The RF current through each coil was measured using a Pearson model 2877 current monitor. L_1, L_2, k_m, and Z_{C1} were measured to be 11.8 μH, 11.8 μH, -0.11, and 14.0 Ω respectively. *Coupled Network Analyzer:* To perform the desired measurements, we constructed a customized instrument called the coupled network analyzer (CNA) which performs the equivalent of an Open Loop Active Load Pull [4]. The CNA generated two simultaneous RF carriers and sampled two RF current inputs simultaneously, with arbitrary phase offsets. The CNA also included several analog and digital I/O, allowing it to vary and measure the V_D and I_D applied to both amplifiers. This allowed for fast quantification of complex coil current and DC power delivery in both channels over the full control space of V_{D1}, V_{D2}, and phase offset φ. Fig 2 shows a block diagram of the experimental setup using the CNA.

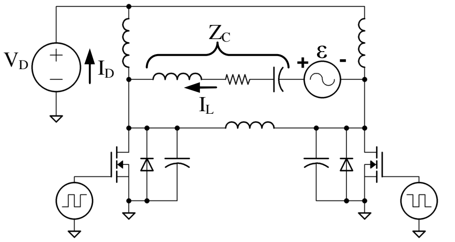

Figure 1: Simplified schematic of the CMCD model, including coil EMF ε from coupling.

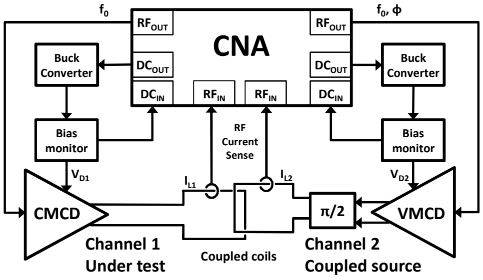

Figure 2: Block diagram of the experimental setup

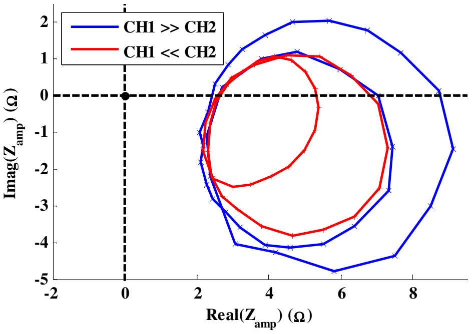

Figure 3: Plots of complex Z_{amp} over phase range φ, for two extreme biasing conditions

Results: To show the measured behavior of the amplifier under test, we reduced the dataset to two extreme cases. In one case, the bias of CH1 was much greater than that of CH2, and in the other case the bias of CH1 was much lower than that of CH2. Fig 3 shows plots of the complex Z_{amp} as a function of phase for both biasing conditions. Fig 4 shows the power transfer through CH1, and its effective drain efficiency, as a function of phase for each biasing condition. The data for each plot takes less than ten seconds to acquire.

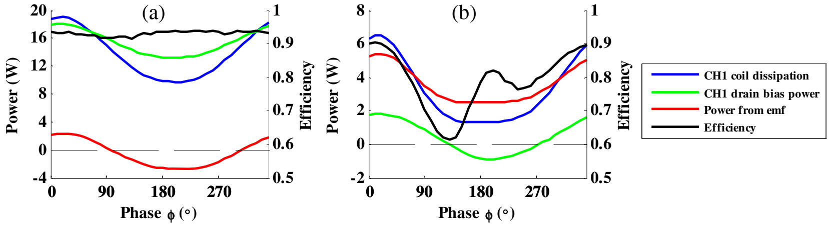

Figure 4: Measured real power flow and effective drain efficiency in the CMCD over full phase range for biasing conditions CH1 ≫ CH2 (a) and CH1 ≪ CH2 (b). Effective drain power was defined as $\eta=P_{coil}/(P_{drain}+P_{emf})$. The negative excursion of CH1 drain bias power in (b) shows the ability of the CMCD to recover coupled power.

Discussion and conclusion: The Z_{amp} measurements shown in fig 3 demonstrate three significant traits of the CMCD output impedance. First, Zamp was found to be a complex function of both bias voltages and phase. Second, Z_{amp} was bounded within a relatively small range, and therefore it may be feasible to apply impedance transformation networks to optimize the impedance seen at the coil. Third, Z_{amp} always occupied the open right half plane, meaning that the amplifier was open loop stable under all conditions. The power measurements shown in fig 4 also demonstrated that when the coupled ε is large compared to the drive level of the CMCD amplifier, the CMCD effectively commutated the induced current back into the DC bias supply, resulting in the incident power being partially recovered, rather than dissipated. It should be noted that this methodology can apply to any amplifier topology, making it useful for development of arrays based on other SMPA topologies or LPA topologies utilizing envelope tracking.

Acknowledgements: This work was supported by Siemens healthcare.

References: [1] Twieg M et al, ISMRM 2012. [2] Gudino N et al, MRM 2013. [3] Roemer et al, MRM 1990. [4] Microwaves 101 - Load Pull for Power Devices [online].